Postprint of: Chróścielewski J., Ferenc T., Mikulski T., Miśkiewicz M., Pyrzowski Ł., Numerical modeling and experimental validation of full-scale segment to support design of novel GFRP footbridge, Composite Structures, Vol. 213 (2019), pp. 299-307, DOI: 10.1016/j.compstruct.2019.01.089



# Numerical modeling and experimental validation of full-scale segment to support design of novel GFRP footbridge

Jacek Chróścielewski[1] ,Tomasz Ferenc[1]*, Tomasz Mikulski[2], Mikołaj Miśkiewicz[1], Łukasz Pyrzowski[1]

[1]Faculty of Civil and Environmental Engineering, Gdansk University of Technology

[2]Faculty of Ocean Engineering and Ship Technology, Gdansk University of Technology

*tomasz.ferenc@pg.edu.pl

Abstract:

The paper contains analysis of full-scaled three meters long segment of a novel composite footbridge. Both numerical modeling and experimental validation were performed. Analyzed object is a shell type sandwich channel-like structure made of composite sandwich with GFRP laminates as a skin and PET foam as a core. Several static load schemes were performed including vertical and horizontal forces. In FEM analysis multilayered laminate was modeled by means of Equivalent Single Layer (ESL) method while the foam was assumed as three-dimensional continuum. Results were compared with the ones obtained from experiments. Good agreement in comparison showed the correctness of conducted assumption what was a great support in designing process of fourteen-and-half meters long footbridge.

## Introduction

The civil engineering industry is still mostly based on traditional materials like steel, concrete or wood. However, in order to meet the increasing requirements for new and more and more challenging structures new solutions are constantly developed. On the one hand structures are desired to be greater, more durable and reliable together with decreasing cost, but on the other hand requirements for material itself are more demanding – its strength has to be higher together with decreasing mass. To fulfill this needs Fiber Reinforcement Polymers (FRP) with their properties are becoming more and more attractive for architects and designers [1]-[5], especially in bridge applications [6]-[8].

The first applications of FRP in the civil engineering industry were mostly focused on strengthening and retrofitting of existing structures [6]. The first FRP structural components in bridge realizations were produced using the basic wet layup process, e.g. the first FRP deck in Miyun Bridge (China) erected in 1982 [9]. The subsequent and up till now the most common in application are structural elements which work unidirectionally manufactured in pultrusion process [10]. Those elements have main strengthening reinforcement oriented unidirectionally which leads to its high longitudinal strength properties and relatively low transversal ones. Such profiles may partially or completely substitute conventional ones in truss or suspension structures. The examples of this kind of application may be find in [11]-[14]. The last decade shows, that manufacturing with the use of other techniques, taken from marine, aviation and automotive industries, becomes to be more popular, e.g. liquid molding processes. The use of such techniques resulted in much greater freedom in shaping geometry of structures or their components. It also allows combining materials in so-called sandwiches where light filler creates

distance between two FRP laminates (skins) and preclude the need of joints use. The examples of such applications may be find in [15]-[19].

In response to the above mentioned experiences, in 2013 the project called FOBRIDGE was created, see [20], (NCBiR grant, number PBS/B2/6/2013, Gdansk University of Technology - Project Leader, Military University of Technology, Roma Private Limited Company - footbridge manufacturer). Its aim was to design, manufacture and investigate single span all-composite foot-and-cycle bridge with channel cross-section and with span length from 12 to 16 meters. Designed footbridge was assumed as a shell, sandwich structure with U-shape cross-section. The object was planned to be repeatable, easy to manufacture in one vacuum infusion process as a single element. The manufacture duration and the cost including exploitation should be competitive to structures made of traditional materials. Additional advantage is the fact that the core of sandwich structure was assumed to be made of a PET foam (polyethylene terephthalate). It gives possibility to apply eco-friendly recycled materials to a footbridge structure during potential mass production [21]. The project assumed building a footbridge from a scratch, so as in the case of all innovative structures, it encountered the following difficulties: guidelines absence in existing design codes, lack of cataloged material data and lack of established modeling principles. Furthermore, mechanical properties of FRP laminates and sandwich structures depend on various parameters: kind of resin [22], the amount and orientation of reinforcement and their cooperation, cooperation of a core with skins, as well as manufacturing techniques and post-cure processes [23], [24]. To overcome these difficulties, it is necessary to extend experimental and numerical analyses often combining both with a validation process, as in [25]-[31] where panels or columns were investigated due to several load schemes. In [25] sandwich columns with various foam core density under axial loading were examined. In [26] sandwich panels with thought-thickness fiber insertions were analyzed and results were compared with non-linear analysis conducted on FEM

model built of solid elements. Paper [27] consist of analysis of panels with various foam cores and ribs – small-scale experimental results (i.e. compressive and tensile tests or tree- and four-point bending) were compared with the one obtained from FEA for models created by means of solid elements as well, and likewise in analysis presented in [28] where panels consist of MgO facings and polystyrene core were studied. In [29] bending of sandwich panels with various insertions were examined - FEM numerical model was created with solid elements for foam core and shell elements for laminated skins. Papers [30] and [31] present experimental and numerical analysis of thin-walled composite columns due to compressive loading – nonlinear problem of stability was solved, the FEM model was built of shell elements. Moreover, standard designing procedures can be extended by conducting e.g. sensitivity analysis [32] and optimization [33], [34], or by failure mode determination i.e. delamination in laminate [35].

For this reason, the experimental research program of the project included identification tests on laminate coupons and foam samples, as well as numerous validation tests, from small structures [36] to the segment with full-scaled cross-section, which is the main topic of this article. The segment was manufactured as three meters long structure using the same design, mold and vacuum infusion technology as prepared for the target footbridge. The reduced length of analyzed object allowed it to be placed in the laboratory, and hence to conduct various static load test schemes. The main aim of analysis was to conduct experimental test which let to validation of numerical model and to check correctness of design assumptions. Furthermore, because of the segment asymmetry, conducted test were to indicate method of strengthening support zone and handrail.

## Description of segment

The analyzed segment is a shell type sandwich structure with U-shape cross-section. The usable width is 2.5 meters as for pedestrian and cycle traffic and the handrail height is 1.3 meters in order to fulfill safety requirement for bridge structure to be erected over train lane (Fig. 1). Total length of structure was reduced compared to the target footbridge up to 3 meters. Such decision was made in order to place the object in laboratory conditions. This gave the opportunity to conduct a greater range of experimental test, as well as to reduce costs. Furthermore, segment was manufactured on target mold and its production was also technological test, hence assumed length was reasonable.

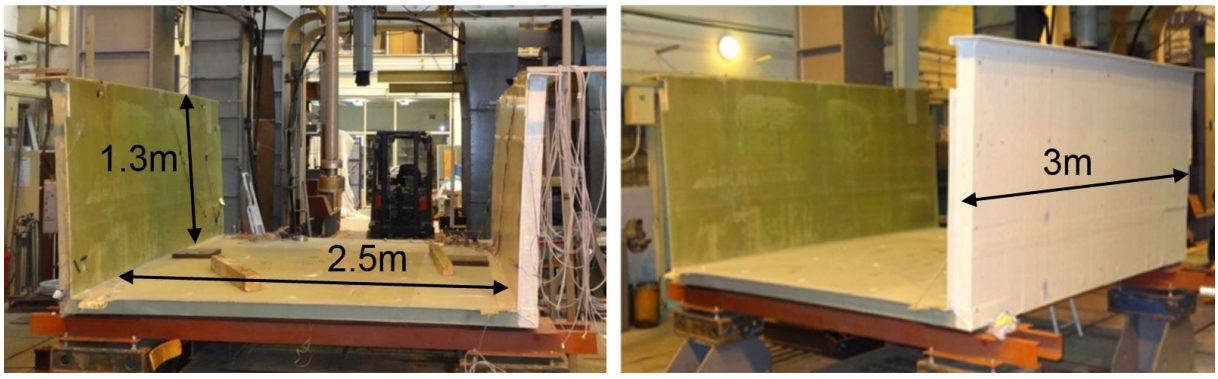


Fig. 1. Geometry of analyzed segment

The segment is a sandwich structure (Fig. 2).The core is made of PET foam with density 100 kg/m$^3$. Multilayered GFRP laminate has glass fibers reinforcement and polymer (vinyl ester) resin constitutes skins. Two types of stitched and balanced fabrics were used: BAT and GBX with fiber directions [0/90] and [+45/-45] respectively, both with density 800 g/m$^2$. Stack sequence is as follows [BAT/GBX/BAT/BAT/GBX/BAT] and is locally disturbed due to longitudinal and transversal ribs. In support zones, instead of PET foam, strengthening blocks are used: composite block in support 1 and wooden block in support 2. Additionally, the cross-

section lips in wall (a) are enhanced with additional foam. Hence, two variants of support zone and two wall cross-section lips were investigated.

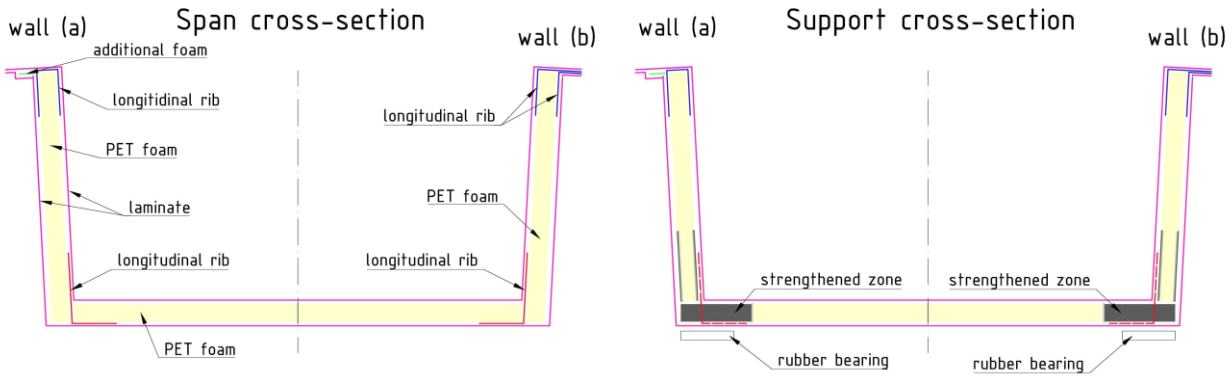


Fig. 2. Cross-section schemes

Material properties of single FRP layer with thickness 0.663 mm and density 1.71 g/cm$^3$was identified by Military University of Technology in temperature 20 °C [37]. A single lamina was assumed as homogenous and orthotropic material with parameters listed in Table 1.

Table 1. Material parameters of single GFRP lamina

| Parameter | | Description | value | unit |
|---|---|---|---|---|
| $E_1$ | $E_2$ | longitudinal (1) and transverse (2) elastic moduli | 23.4 | [GPa] |
| $v_{12}$ | | Poisson's ratio | 0.153 | [-] |
| $G_{12}$ | | in-plane shear modulus | 3.52 | [GPa] |
| $G_{13}$ | $G_{23}$ | transverse shear moduli | 1.36 | [GPa] |
| $X_t$ | $Y_t$ | longitudinal (1) and transverse (2) strength in tension | 449 | [MPa] |
| $X_c$ | $Y_c$ | longitudinal (1) and transverse (2) strength in compression | 336 | [MPa] |
| $S$ | | in-plane shear strength | 45.2 | [MPa] |
| $S_t$ | | transverse shear strength | 34.7 | [MPa] |

Properties of PET foam were delivered by a producer. Finally, for designing purpose only, parameters were assumed as for PET foam with density 100 kg/m$^3$. Hence homogenous isotropic material was taken into consideration with the characteristics listed in Table 2.

Additional composite blocks near support zone 1 was modeled using homogenous and orthotropic solid material with parameters listed in Table 3, while wooden block near support

zone 2 using homogenous isotropic material with the following characteristics: elastic modulus $E$ = 6 GPa and Poisson's ratio $v$ =0.3.

Table 2. Material parameters of PET foam

| Parameter | Description | value | unit |
|---|---|---|---|
| $E$ | elastic modulus | 70 | [MPa] |
| $v_{12}$ | Poisson's ratio | 0.4 | [-] |
| $R_t$ | strength in tension | 2.7 | [MPa] |
| $R_c$ | strength in compression | 1.8 | [MPa] |

Table 3. Material parameters of composite block

| Parameter | | Description | value | unit |
|---|---|---|---|---|
| $E_1$ | $E_2$ | longitudinal (1) and transverse (2) elastic moduli | 8.25 | [GPa] |
| $E_3$ | | transverse (3) elastic modulus | 4.15 | [GPa] |
| $v_{12}$ | | in-plane Poisson's ratio | 0.39 | [-] |
| $v_{23}$ | | transverse (23) Poisson's ratio | 0.235 | [-] |
| $v_{31}$ | | transverse (31) Poisson's ratio | 0.118 | [-] |
| $G_{12}$ | | in-plane shear modulus | 3.04 | [GPa] |
| $G_{13}$ | $G_{23}$ | transverse shear moduli | 3.1 | [GPa] |

The three meters long segment was installed onto four squared rubber bearings with dimensions of 30 x 30 x 3 cm. Material was assumed as homogenous and isotropic with elastic modulus $E$ = 12.58 GPa and Poisson's ratio $v$ =0.48. Each support was assumed as fixed only in vertical direction.

## Load schemes an test set-up

Several load schemes were designed in order to investigate as accurately as possible behavior of the structure (Table 4 and Fig. 3). The first load group designated as A consists of four load schemes: A3, A4, A6 and A7, where vertical load was applied either on platform or on the top of walls and was generated by hydraulic cylinder (Fig. 3a-d). Their aim was to simulate usable traffic loading, however instead of area loading, point forces were applied. Despite easiness of conducting in the laboratory conditions, they give higher material effort and especially in

sandwich structures are more dangerous due to debonding problem. Moreover, target footbridge is also designed to provide ambulance passage (concentrated forces caused by wheels). The other load types: B (B1 and B2) and C (Ca and Cb) was executed by means of fixing steel elements and rods. The total force was generated by turnbuckles and measured by strain gauges installed on single (in schemes B) or both (in schemes C) rods (Fig. 3e-f). The aim of load schemes B was to simulate walls bending over each support, while load schemes C were conducted to simulate compression of the top of walls in order to investigate whether buckling of walls or handrail occur.

Table 4. Conducted load schemes

| Load scheme | Description | Load value |
|---|---|---|
| A3 | Two forces applied on deck near walls in the middle of span | 80 kN totally |
| A4 | Single force in the middle of decks width in the middle of span | 50 kN |
| A6 | Two forces applied halfway the width of the deck at a spacing of 2 meters | 50 kN totally |
| A7 | Single force in the middle of decks width over support no 1 | 50 kN |
| B1 (B2) | Horizontal force applied transversally over support no 1 (2) | 12.5 (9.2) kN |
| Cb (Ca) | Horizontal force applied longitudinally along wall b (a) | 100 kN |

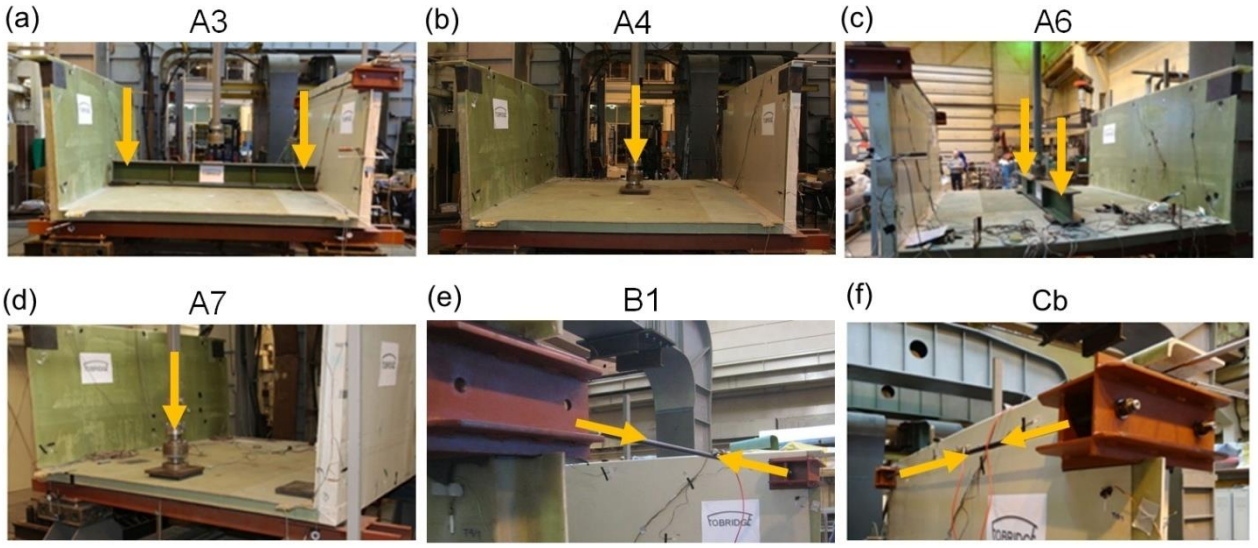


Fig. 3. Load schemes

The values of applied forces was assessed based on pre-calculations in order to obtain extreme stress level that can occur for target footbridge designing according to the polish codes. Compression of handrails due to traffic loading of the target footbridge with 14 meters span-length correspond with conducted schemes C, also point loadings applied on deck (schemes group A) are similar to the one that occur due to ambulance passage or is total force computed from standard area loading. Hence, stress level in each structural element was investigated. Extreme load values were estimated by controlling stress level in laminates layers and foam separately.

Stress level in a single orthogonal layer of laminate was controlled by means of Failure Index (FI) according to Tsai-Wu hypothesis [38]:

$$FI = F_1\sigma_1 + F_{11}\sigma_1^2 + F_2\sigma_2 + F_{22}\sigma_2^2 + 2F_{12}\sigma_1\sigma_2 + F_{66}\tau_{12}^2, \quad (1)$$

where constants $F_i$ or $F_{ij}$ are given by

$$F_1 = \frac{1}{X_t} - \frac{1}{X_c}, \quad F_2 = \frac{1}{Y_t} - \frac{1}{Y_c}, \quad F_{11} = \frac{1}{X_t X_c}, \quad F_{22} = \frac{1}{Y_t Y_c}, \quad F_{66} = \frac{1}{S^2}, \quad F_{12} = F_{12}^* \sqrt{F_{11}F_{22}}. \quad (2)$$

Constant $F_{12}$ is user-defined interaction coefficient with additional coefficient $F_{12}$* assessed at level 0.5 [39].

For the purpose of object designing [40], [41] the Thai-Wu FI was assessed at level up to ~0.2 in laminate and the ratio of unidirectional stress to strength in tension or compression at level up 0.8 in foam. The FI value (~0.2) was assumed due to the prevention of microcracks that occur in biaxially strengthened laminates which are used in designing object. Consequently, when the FI value is higher than assumed value, there is a point where elastic properties decrease. Fig. 4 presents the example of uniaxial tensile experiment conducted on five specimens for four layered laminate with stack sequence as follows [BAT/GBX/ GBX/BAT]. At strain level about 0.005 material parameters change their value. According to ISO 527-1 parameters are determined in the

range of strain from $\varepsilon_1$ = 0.0005 to $\varepsilon_2$ = 0.0025 (vertical dashed red lines on Fig. 4), so before microcracks occur.

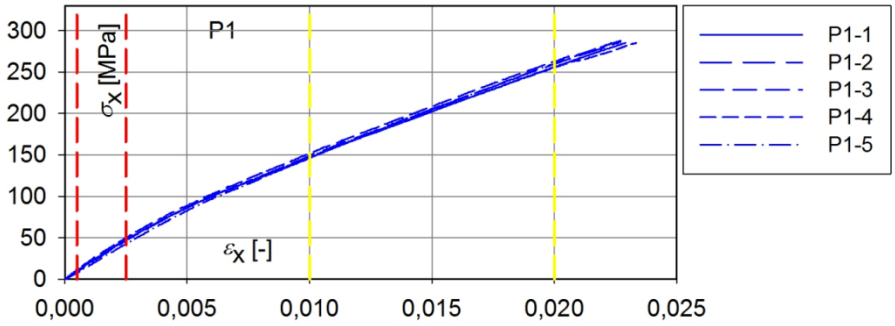


Fig. 4. Stress-strain relation in biaxially strengthened laminate

The following instrumentation was installed and used during experiments:

- 60 electrical resistive strain gauges (Fig. 5a) denoted as Tx/y, with base 20 mm and electrical resistance 120 Ohm, with HBM Data Acquisition System MX 1615
- 14 inductive sensors HBM WA100 (Fig. 5b) for measuring displacements denoted as Ux/y, with HBM Data Acquisition System MX 840A
- 4 dial gauges (Fig. 5c) for measuring displacements near support zones denoted as Ox and measuring bearings shortening
- 2 strain gauges to measure force in system of rods used in schemes B and C.

Location of strain gauges T, inductive sensors U and dial gauges O is presented in Fig. 6.


Fig. 5. Measuring equipment: (a) strain gauge, (b) inductive sensor, (c) dial gauge

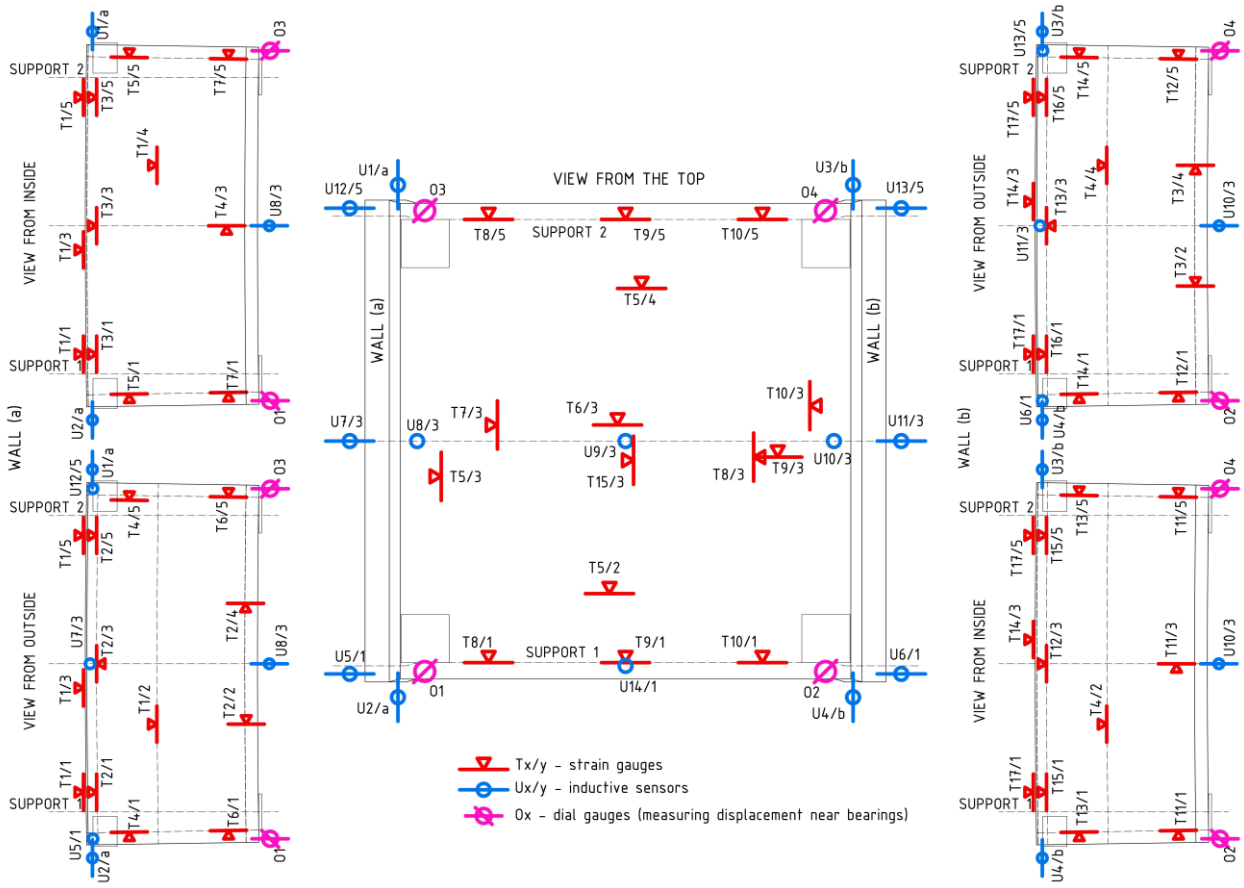


Fig. 6. Localization of measuring points

## Numerical modeling

Numerical simulations of analyzed structure were performed in FEMAP with Nastran environment. The aim of numerical modelling is to represent behavior of a real structure. Considering composite structures several methods are available: three dimensional (3D) continuum formulations, or two dimensional (2D) continuum with reduction of dimension related to thickness: Layerwise modeling (LW) and Equivalent Single Layer (ESL) [42]-[44]. The first method 3D is the most complex and accurate, but on the other hand the least effective. The simplified 2D methods are used more widely, the first one LW takes into account each layers of

laminate, the second ESL treats laminate as one layer. Selection of an appropriate method depends on the geometry of the structure, as well as the desired accuracy of the results.

Due to desired accuracy and the range of deformation that occur during conducted experiments combine method of modeling was chosen. Laminated skins of sandwich were modeled by means of ESL approach with First Order Shear Deformation Theory (FOSD or FSDT) with shear correction factor estimated numerically while core foam was modeled as solids. Hence four nodes shell finite elements were used as a representation of laminate with linear shape functions and full integration. The foam core was considered as 3D continuum and was modelled by means of eight node solid finite elements with linear shape functions and full integration as well. Both elements, laminate and foam, was modelled as linear material due to assumed strain/stress level. Numerical model (Fig. 7) consists of 155779 nodes and 227082 elements totally, while in Table 5 list with number of each type of element used in the model are presented.

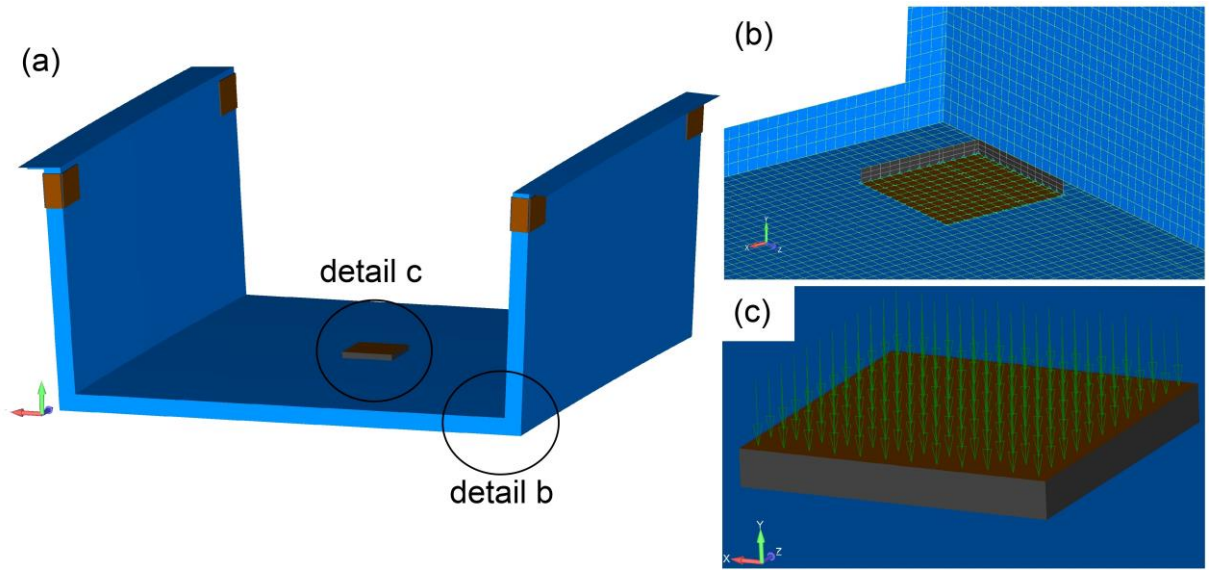


Fig. 7. Visualization of numerical model: (a) overall view, (b) detail of rubber bearing with mesh size, (c) detail of applied load

Table 5. Elements used in FEM model

| Item | Element type | Number |
|---|---|---|
| Laminate | Four nodes shell element<br>with full integration and linear shape function | 99450 |
| Foam | Eight nodes solid element<br>with full integration and linear shape function | 117936 |
| Rubber | Eight nodes solid element<br>with full integration and linear shape function | 7272 |
| Steel elements | Four nodes shell element<br>with full integration and linear shape function | 2424 |
| | sum | 227082 |

A regular fine mesh was built assuming the distance between nodes as about 25 mm, it gives four or five finite element through the thickness of sandwich structure (see Fig. 7b). The correctness of the mesh adoption was confirmed by the convergence test. The experimental tests did not contain large deformation and destructive tests, therefore all analyses were limited to linear static calculations. In the numerical analysis loads were applied analogously to the experiment, i.e. through steel elements and rubber pad, e.g. for scheme A4 load was set as presented on Fig. 7c.

## Comparison of FEA and experimental results

The results obtained in numerical analyses are compared with the experimental ones in representatives points. For each conducted scheme several point were chosen to compare value received from model and experiment. For schemes group A point near applied force were analyzed, mainly on segments platform, in mid-span cross-section (for A3 and A4) or support cross-section (for A7). For scheme B1 points located near support 1 cross-section on both walls and platform were taken into account, while for scheme Cb points that lie along wall (b) were analyzed.

## Model validation

The first comparison of results did not meet expectations. Relative errors exceed high values, especially analyzing deformations near support zones. In order to obtain higher accuracy, material parameters of rubber bearings were updated by comparison vertical displacement in support zones obtained from sensors O1, O2, O3, O4 (see Table 6). Moreover, numerical model seemed to be less stiff than real structure. This was due to the fact that, despite longitudinal ribs presented on Fig. 2, real structure had also transversal ribs which were C- or H-shape. They had an extra margin for better connection with face sheets. Therefore, in the vicinity of the ribs, the stacking of the structure skins was enriched by extra layers. In the first approach that extra margin was omitted, however after model validation they were taken into account (Fig. 8).

Table 6. Updated elastic moduli of rubber bearings

| Sensor | Updated elastic modulus [MPa] | Displacement in experim. [mm] | Displacement in model [mm] |
|---|---|---|---|
| O1 | 0,63 | 1,36 | 1,41 |
| O2 | 0,64 | 1,40 | 1,40 |
| O3 | 0,7 | 1,16 | 1,23 |
| O4 | 0,85 | 0,99 | 1,03 |

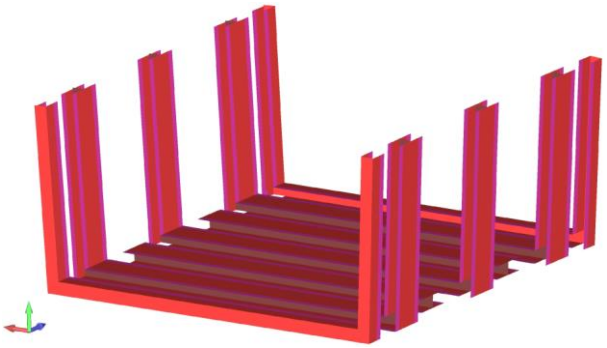

Fig. 8. Transversal ribs taken into account after validation

Comparisons of the results after model validation are listed in Table 7-Table 12 including relative error determination. Additional visualizations of results are presented on Fig. 9-Fig. 14, where comparison of chosen deformation are presented. Additionally, on Fig. 9b-Fig. 12b history of applying force is shown.

## Scheme A3

Table 7. Scheme A3: Values in points

| point | experim. | model | error |
|---|---|---|---|
| strains [μm/m] | | | |
| T1/3 | -136 | -124 | -9,3% |
| T4/3 | 438 | 467 | 6,3% |
| T5/3 | 132 | 137 | 3,6% |
| T6/3 | 134 | 119 | -12,2% |
| T7/3 | 116 | 148 | 21,6% |
| T9/3 | 475 | 565 | 16,0% |
| T11/3 | 457 | 469 | 2,7% |
| T14/3 | -145 | -134 | -7,8% |
| displacements [mm] | | | |
| U7/3 | -5,64 | -4,46 | -26,3% |
| U8/3 | 2,72 | 2,53 | -7,3% |
| U9/3 | 5,92 | 5,95 | 0,6% |
| U10/3 | 2,07 | 2,46 | 16,1% |
| U11/3 | -6,10 | -4,75 | -28,4% |

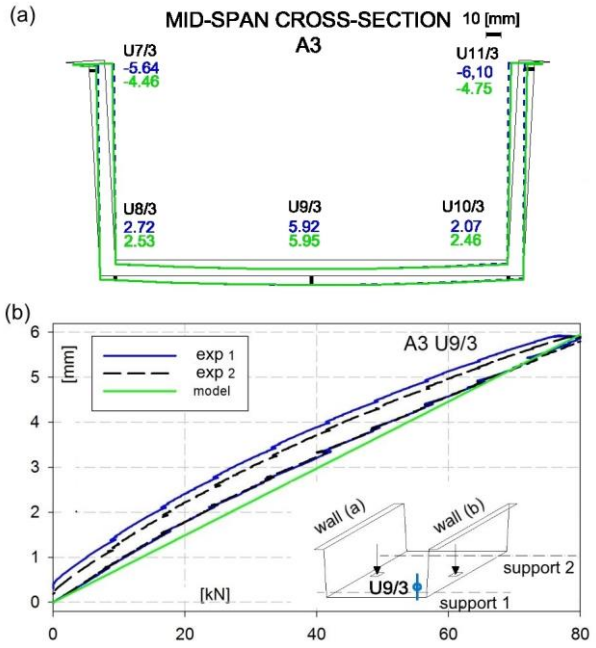


Fig. 9. A3: (a) deformed cross-section, (b) displacement U9/3

## Scheme A4

Table 8. Scheme A4: Values in points

| point | experim. | model | error |
|---|---|---|---|
| strains [μm/m] | | | |
| T9/1 | 668 | 545 | -22,6% |
| T5/2 | 605 | 627 | 3,6% |
| T5/3 | 121 | 112 | -7,6% |
| T6/3 | 1240 | 1451 | 14,6% |
| T8/3 | 167 | 213 | 21,6% |
| T9/3 | 118 | 113 | -4,0% |
| T15/3 | 835 | 641 | -30,3% |
| T5/4 | 640 | 622 | -2,8% |
| T9/5 | 585 | 549 | -6,5% |
| displacements [mm] | | | |
| U7/3 | -11,10 | -12,6 | 11,9% |
| U8/3 | 1,96 | 0,98 | -99,5% |
| U9/3 | 14,60 | 16,27 | 10,3% |
| U10/3 | 1,42 | 1 | -41,5% |
| U11/3 | -11,21 | -12,86 | 12,8% |

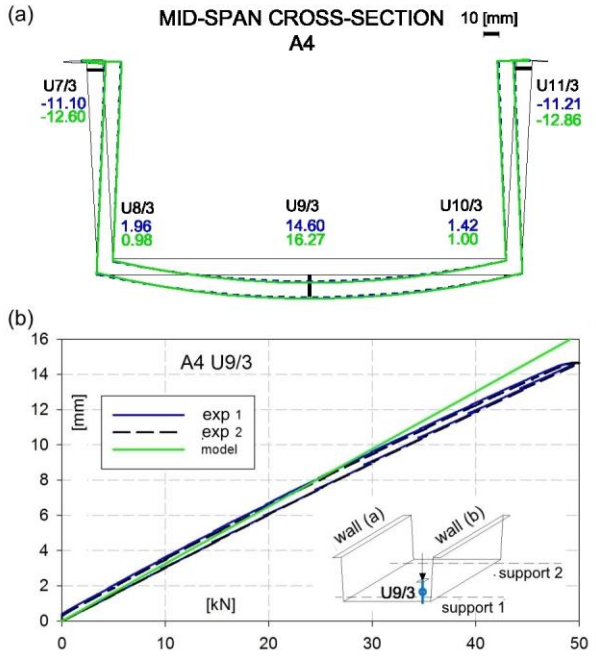


Fig. 10. A4: (a) deformed cross-section, (b) displacement U9/3

## Scheme A6

Table 9. Scheme A6: Values in points

| point | experim. | model | error |
|---|---|---|---|
| strains [μm/m] | | | |
| T9/1 | 2009 | 1807 | -11,2% |
| T5/2 | 1762 | 2088 | 15,6% |
| T6/3 | 1064 | 1186 | 10,3% |
| T6a/3 | 969 | 1185 | 18,3% |
| T9/3 | 383 | 477 | 19,7% |
| T5/4 | 2654 | 2111 | -25,7% |
| T9/5 | 1830 | 1848 | 1,0% |
| displacements [mm] | | | |
| U7/3 | -23,02 | -28,53 | 19,3% |
| U8/3 | 2,35 | 1,2 | -95,4% |
| U9/3 | 16,63 | 18,43 | 9,8% |
| U10/3 | 1,59 | 1,2 | -32,5% |
| U11/3 | -23,32 | -28,99 | 19,6% |

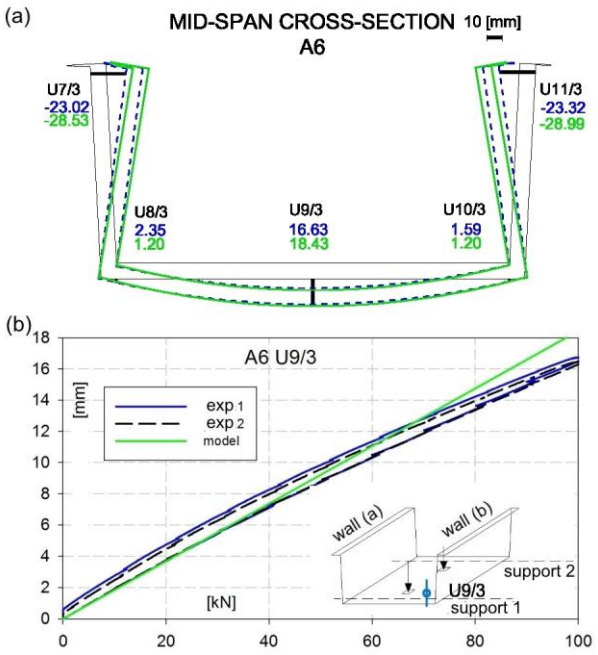


Fig. 11. A6: (a) deformed cross-section, (b) displacement U9/3

## Scheme A7

Table 10. Scheme A7: Values in points

| point | experim. | model | error |
|---|---|---|---|
| strains [μm/m] | | | |
| T6/1 | -232 | -220 | -5,2% |
| T7/1 | 209 | 265 | 21,1% |
| T9/1 | 2443 | 2331 | -4,8% |
| T11/1 | 225 | 264 | 14,8% |
| T12/1 | -222 | -220 | -0,7% |
| T5/2 | 1273 | 1523 | 16,4% |
| T6/3 | 479 | 507 | 5,5% |
| displacements [mm] | | | |
| U5/1 | -16,69 | -21,6 | 22,8% |
| U6/1 | -17,80 | -21,78 | 18,3% |
| U14/1 | 23,21 | 26,53 | 12,5% |

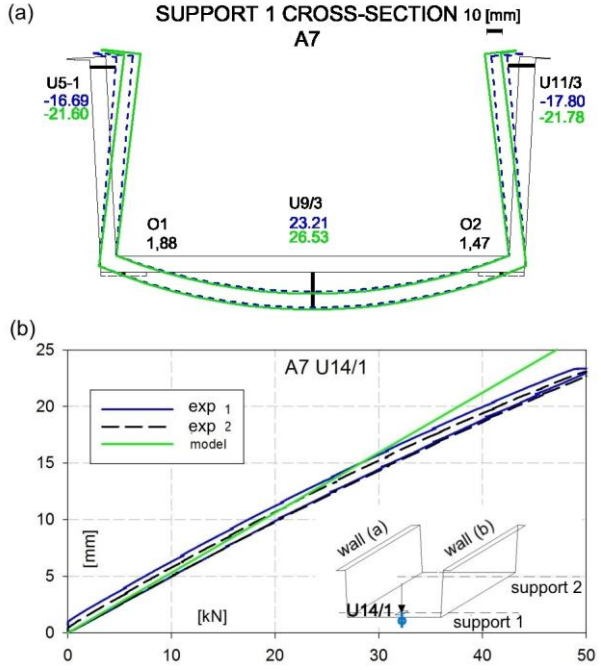


Fig. 12. A7: (a) deformed cross-section, (b) displacement U14/1

## Scheme B1

Table 11. Scheme B1: Values in points

| point | experim. | model | error |
|---|---|---|---|
| strains [μm/m] | | | |
| T6/1 | 856 | 732 | -16,9% |
| T7/1 | -732 | -713 | -2,7% |
| T8/1 | 876 | 762 | -15,0% |
| T9/1 | 683 | 588 | -16,1% |
| T10/1 | 790 | 760 | -3,9% |
| T11/1 | -762 | -720 | -5,8% |
| T12/1 | 847 | 737 | -14,9% |
| T5/2 | 491 | 493 | 0,5% |
| displacements [mm] | | | |
| U5/1 | -39,13 | -37,71 | -3,8% |
| U6/1 | -37,33 | -38,06 | 1,9% |
| U7/3 | -24,24 | -25,1 | 3,4% |
| U11/3 | -24,23 | -24,98 | 3,0% |
| U12/5 | -16,35 | -16,81 | 2,7% |
| U13/5 | -17,82 | -17,14 | -3,9% |

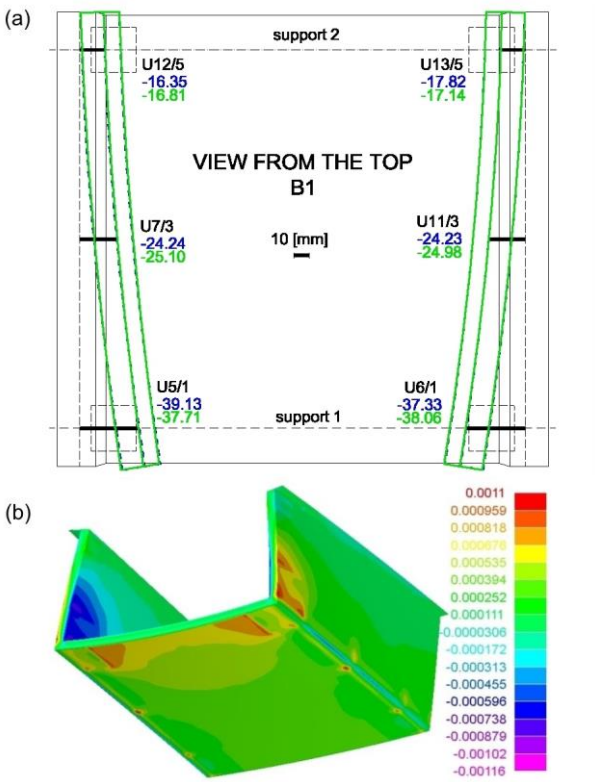


Fig. 13. B1: (a) view from the top of deformed structure,
(b) visualization of transversal strains of deformed structure

## Scheme Cb

Table 12. Scheme Cb: Values in points

| point | experim. | model | error |
|---|---|---|---|
| strains [μm/m] | | | |
| T15/1 | -936 | -730 | -28,2% |
| T16/1 | -319 | -551 | 42,1% |
| T17/1 | -653 | -724 | 9,7% |
| T12/3 | -623 | -572 | -9,0% |
| T13/3 | -473 | -496 | 4,7% |
| T14/3 | -552 | -624 | 11,6% |
| T15/5 | -800 | -733 | -9,2% |
| T16/5 | -333 | -552 | 39,8% |
| T17/5 | -671 | -724 | 7,4% |
| displacements [mm] | | | |
| U3/b | -0,66 | -1,01 | 34,4% |
| U4/b | -1,00 | -0,98 | -1,3% |
| U6/1 | -1,92 | -0,54 | -257,1% |
| U11/3 | 1,99 | 0,56 | 254,7% |
| U13/5 | -1,69 | -1,01 | -67,9% |

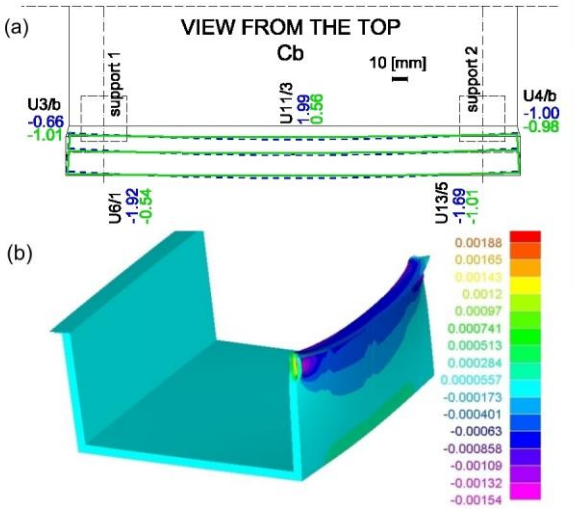


Fig. 14. Cb: (a) view from the top of deformed structure
(b) visualization of longitudinal strains of deformed structure

**Discussion**

Conducted experiments allow to determine the level of strains and displacements due to several load schemes of the structure of composite sandwich segment. Obtained values were then compared to the FEM analysis ones and, as it was shown, the error in representatives points was about 5-20%. More significant difference between in situ tests and FEM numerical simulations may be caused by a few reasons. In points where measured values are small the relative error become higher. Some values highly depends on the way how the load was applied. To assure correspondence between experiment and FEM analysis the force was applied as a uniformly distributed load in area of 30x30 cm (Fig. 7c). Some incompatibility between results may be caused by nonlinear dependence of measured valued in the function of applied force, like displacement obtained in sensor U9/3 in conducted load scheme A3 or A4 which are shown in Fig. 9b and Fig. 10b. This may occur due to nonlinear contact between segment and rubber bearings or because of its nonlinear behavior oneself. Is also has to be mentioned that no buckling occur while handrail compression is scheme C.

Despite this, the method of combined modeling of sandwich composite structure with multilayered laminate as a single layered shell according to ESL theory and core foam by means of solid elements seems to be effective. The behavior of structure is properly simulated with sufficient accuracy. Hence the combined method, the type of used finite elements may be used to analyzed target composite footbridge.

Furthermore, conducted tests were aimed at selecting the strengthening method of support zone and handrail. Both solutions gave satisfying results,. No damage symptoms was revealed near support zone, either no buckling occur in handrail. For target footbridge realization variant with composite block in support zone and no additional foam in handrail was chosen.

## Final remarks

Experimental validation test and numerical simulations of full-scaled cross-section segment of composite sandwich footbridge with GRP skins and PET foam were presented in the paper. In situ measured values of strains and displacements in the most representative points are in good agreement with FEM numerical results. Although numerical model validation is a complicated process due to complexity of the structure, conducted actions shown, that the behavior of segment is simulated correctly by means of combined modeling in which multilayered laminates are substituted by single layered shell according to ESL theory and foam stays as three-dimensional continuum.

Conducted validation and results comparison gave confirmation of the assumptions made while FE model analysis of an innovative composite sandwich structure. The conclusions drawn from the presented analysis were used as one of the steps supporting the FOBRIDGE project in constructing of a target footbridge. The structure was designed, manufactured and then erected in the campus of Gdansk University of Technology (Poland) and investigated for nearly one year time including both static [45] and dynamic loadings [46].

## Acknowledgment

The study was supported by the National Centre for Research and Development, Poland, grant no PBS1/B2/6/2013.

## References

[1] Correia, J. R. (2014). Fibre-Reinforced Polymer (FRP) Composites. Materials for Construction and Civil Engineering, 501–556. doi:10.1007/978-3-319-08236-3_11.

[2] Manalo, A., Aravinthan, T., Fam, A., & Benmokrane, B. (2017). State-of-the-Art Review on FRP Sandwich Systems for Lightweight Civil Infrastructure. Journal of Composites for Construction, 21(1). doi:10.1061/(asce)cc.1943-5614.0000729.

[3] Hollaway, L. C. (2010). A review of the present and future utilisation of FRP composites in the civil infrastructure with reference to their important in-service properties. Construction and Building Materials, 24(12), 2419–2445. doi:10.1016/j.conbuildmat.2010.04.062

[4] Keller, T., Haas, C., &Vallée, T. (2008). Structural Concept, Design, and Experimental Verification of a Glass Fiber-Reinforced Polymer Sandwich Roof Structure. Journal of Composites for Construction, 12(4), 454–468. doi:10.1061/(asce)1090-0268(2008)12:4(454).

[5] Sharaf, T., & Fam, A. (2011). Experimental Investigation of Large-Scale Cladding Sandwich Panels under Out-of-Plane Transverse Loading for Building Applications. Journal of Composites for Construction, 15(3), 422–430. doi:10.1061/(asce)cc.1943-5614.0000176.

[6] Potyrała, P. B. & Rius, J. R. C. (2011). Use of fibre reinforced polymer composites in bridge construction. State of the Art in Hybrid and All-Composite Structures. Escola Tecnica Superior d'Enginyers de Camins, Canals i Ports de Barcelona. Universitat Politècnica de Catalunya, Departament Enginyeria de la Construcció.

[7] Hollaway, L. C. (2013). Applications of advanced fibre-reinforced polymer (FRP) composites in bridge engineering: rehabilitation of metallic bridge structures, all-FRP composite bridges, and bridges built with hybrid systems. Advanced Fibre-Reinforced Polymer (FRP) Composites for Structural Applications, 631–661. doi:10.1533/9780857098641.4.631

[8] Siwowski T., Kulpa M., Rajchel M., Poneta P. (2018). Design, manufacturing and structural testing of all-composite FRP bridge girder. Composite Structures, 206, Pages: 814-827 , DOI: 10.1016/j.compstruct.2018.08.048

[9] Keller, T. (2002). Overview of Fibre-Reinforced Polymers in Bridge Construction. Structural Engineering International, 12(2), 66–70. doi:10.2749/101686602777965595.

[10] Ascione F., Lamberti M., Razaqpur G. (2015) Modifications of standard GFRP sections shape and proportions for improved stiffness and lateral-torsional stability. Composite Structures 2015, 265-289, 132 doi: 10.1016/j.compstruct.2015.05.005

[11] Sobrino, J. A., &Pulido, M. D. G. (2002). Towards Advanced Composite Material Footbridges. Structural Engineering International, 12(2), 84–86. doi:10.2749/101686602777965568

[12] Braestrup, M. W. (1999). Footbridge Constructed from Glass-Fibre-Reinforced Profiles, Denmark. Structural Engineering International, 9(4), 256–258. doi:10.2749/101686699780481709.

[13] Harvey, W. J. (1993). A Reinforced Plastic Footbridge, Aberfeldy, UK. Structural Engineering International, 3(4), 229–232. doi:10.2749/101686693780607589

[14] Daniel, R. A. (2003). Environmental considerations to structural material selection for a bridge, proceedings of the COBRAE European Bridge Engineering Conference "Lightweight Bridge Decks", March 2003, Rotterdam, Holland.

[15] Santos, F. M. dos, & Mohan, M. (2011). Train Buffeting Measurements on a Fibre-Reinforced Plastic Composite Footbridge. Structural Engineering International, 21(3), 285–289. doi:10.2749/101686611x13049248220087.

[16] Areiza Hurtado, M., Bansal, A., Paulotto, C., &Primi S. (2012). FRP girder bridges: Lessons learned in Spain in the last decade, Proceedings of the 6th International Conference on FRP Composites in Civil Engineering (CICE-6), Rome, Italy.

[17] Siwowski, T., Kaleta, D., & Rajchel, M. (2018). Structural behaviour of an all-composite road bridge. Composite Structures, 192, 555–567. doi:10.1016/j.compstruct.2018.03.042.

[18] Piatek, B. & Siwowski, T (2017). Research on the new CFRP prestressing system for strengthening of RC structures. Architetecture Civl Engrineering Environment. Vol. 10, 3, 81-87

[19] Kulpa M. & Siwowski T. (2018). Stiffness and strength evaluation of a novel FRP sandwich panel for bridge redecking. Composite Part B, 167, 207-220. doi: 10.1016/j.compositesb.2018.12.004

[20] Chróścielewski, J., Miśkiewicz, M., Pyrzowski, Ł. & Wilde, K. (2017). Composite GFRP U-Shaped Footbridge. Polish Maritime Research, 24(s1). doi:10.1515/pomr-2017-0017

[21] Żyjewski, A., Chróścielewski, J. & Pyrzowski Ł. (2017) The use of fibre-reinforced polymers (FRP) in bridges as a favourable solution for the environment. Kaźmierczak B, Kutyłowska M, Piekarska K, Trusz-Zdybek A, editors. E3S Web of Conferences [Internet]. EDP Sciences; doi: 10.1051/e3sconf/20171700102

[22] Pyrzowski Ł (2018) Testing Contraction and Thermal Expansion Coefficient of Construction and Moulding Polymer Composites, Polish Maritime Research, vol. 25, no. s1, pp. 151–158, doi: 10.2478/pomr-2018-0036

[23] Jones R. M. (1999). Mechanics of Composite Materials. Taylor & Francis, London.

[24] Harris B. (1999). Engineering Composite Materials. London

[25] Co Dyre L., & Fam, A. (2016). The effect of foam core density at various slenderness ratios on axial strength of sandwich panels with glass-FRP skins. Composites Part B: Engineering, 106, 129–138. doi:10.1016/j.compositesb.2016.09.016.

[26] Lanssens T., Tanghe C., Rahbar N., Okumus P., Van Dessel S. & El-Korchi T. (2014). Mechanical behavior of a glass fiber-reinforced polymer sandwich panel with through-thickness fiber insertions. Construction and Building Materials, 64, 473–479. doi:10.1016/j.conbuildmat.2014.04.052.

[27] Tuwair, H., Hopkins, M., Volz, J., El Gawady, M. A., Mohamed, M., Chandrashekhara, K., & Birman, V. (2015). Evaluation of sandwich panels with various polyurethane foam-cores and ribs. Composites Part B: Engineering, 79, 262–276. doi:10.1016/j.compositesb.2015.04.023.

[28] Smakosz Ł & Kreja I (2018) Failure mode prediction for composite structural insulated panels with MgO board facings, AIP Conference Proceedings 1922, 050004 doi:10.1063/1.5019058

[29] Dawood, M., Taylor, E., & Rizkalla, S. (2010). Two-way bending behavior of 3-D GFRP sandwich panels with through-thickness fiber insertions. Composite Structures, 92(4), 950–963. doi:10.1016/j.compstruct.2009.09.040.

[30] Debski H, Teter A. (2015) Numerical and experimental studies on the limit state of fibre-reinforced composite columns with a lipped channel section under quasi-static compression. Compososite Structures, 133:1e7. doi: 10.1016/j.compstruct.2015.07.053.

[31] Kubiak T., Mania R.J. (2016). Hybrid versus FR laminate channel section columns – Buckling and postbuckling behaviour. Composite Structures, 154, 142-149, DOI: 10.1016/j.compstruct.2016.07.040

[32] Ferenc T., Pyrzowski Ł., Chróścielewski J. & Mikulski T. (2018) Sensitivity analysis in designing process of sandwich U-shaped composite footbridge, Shell Structures: Theory and Applications. - Vol. 4, ed. W. Pietraszkiewicz, W. Witkowski, Leiden: CRC Press/Balkema, 413-416

[33] Barnes RH, Morozov EV (2016) Structural optimisation of composite wind turbine blade structures with variations of internal geometry configuration. Composite Structures, 152:158–167. https://doi.org/10.1016/j.compstruct.2016.05.013

[34] Malachowski J., Mazurkiewicz L., Damaziak K. & Tomaszewski M. (2018): Evaluation of the response of fibre reinforced composite repair of steel pipeline subjected to puncture from excavator tooth. Composite Structures, 202:1126–1135., DOI:10.1016/j.compstruct.2018.05.065

[35] Khan A., Ko D-K., Lim S.C., Kim H.S.: (2019). Structural vibration-based classification and prediction of delamination in smart composite laminates using deep learning neural network. Composite Part B, 161, 586-594 DOI: 10.1016/j.compositesb.2018.12.118

[36] Pyrzowski, Ł., Sobczyk, B., Witkowski, W., & Chróścielewski, J. (2016). Three-point bending test of sandwich beams supporting the GFRP footbridge design process—validation. Advances in Mechanics: Theoretical, Computational and Interdisciplinary Issues, 489–492. doi:10.1201/b20057-104.

[37] Chróścielewski J, Klasztorny M, Romanowski R, Barnat W, Małachowski J, Derewońko A, et al. (2015) Badania eksperymentalne identyfikacyjne kompozytu. Raport z realizacji podzadania 5.1 WAT (internal report), Warsaw

[38] Tsai S. W. & Wu E. M. (1971) A general theory of strength for anisotropic materials, J. Comp. Mater. 5 (1)

[39] Tsai S. W &, Hahn H. T. (1980) Introduction to composite materials, Technomic Publishing Co., Lancaster, USA

[40] Chróścielewski J, Klasztorny M, Nycz D, Sobczyk B. (2014) Load capacity and serviceability conditions or footbridges made of fibre-reinforced polymer laminates. Roads Bridges;13,189-202. http://dx.doi.org/10.7409/rabdim.014.013

[41] Małachowski J, L'vov G, Daryazadeh S. (2017) Numerical prediction of the parameters of a yield criterion for fibrous composites. Mechanics of Composite Materials, 53, 589–600. http://dx.doi.org/10.1007/s11029-017-9689-1.

[42] Altenbach H., Altenbach J. & Kissing W. (2001) Structural analysis of laminate and sandwich beams and plates, An introduction into the mechanics of composite, Lubelskie Towarzystwo Naukowe, Lublin

[43] Reddy, J. N. (1984) A simple higher-order theory for laminated composite plates, Journal of Applied Mechanics, Trans. ASME, Vol. 51, 745-752

[44] Sabik A. & Kreja I. (2008) Linear analysis of laminated multilayered plates with the application of zig-zag function. Archives of Civil and Mechanical Engineering, 8, 61-72

[45] Chróścielewski J., Miśkiewicz M., Pyrzowski Ł., Sobczyk B. & Wilde K. (2017) A novel sandwich footbridge - Practical application of laminated composites in bridge design and in situ measurements of static response, Composites Part B 126, 153-161

[46] Chróścielewski J., Miśkiewicz M., Pyrzowski Ł., Rucka M., Sobczyk B. & Wilde K (2018) Modal properties identification of a novel sandwich footbridge – Comparison of measured dynamic response and FEA, Composites Part B 151, 245-255